ELSEVIER

Brain & Development 33 (2011) 627–631

BRAIN & DEVELOPMENT
Official Journal of the Japanese Society of Child Neurology

www.elsevier.com/locate/braindev

Review article

Rett syndrome: The state of clinical and basic research, and future perspectives

Toyojiro Matsuishi [a,*], Yushiro Yamashita [a], Tomoyuki Takahashi [b], Shinichiro Nagamitsu [a]

[a] *Department of Pediatrics and Child Health, Kurume University School of Medicine, Kurume 830-0011, Japan*
[b] *Division of Gene Therapy and Regenerative Medicine, Cognitive and Molecular Research Institute of Brain Diseases, Kurume University, Japan*

Received 28 September 2010; accepted 14 December 2010

Abstract

To clarify the pathophysiology of brain and spinal cord impairment in Rett syndrome (RTT), we report on the current status of research on Rett syndrome and review the abnormalities reported in neurotransmitters, neuromodulators and other biological markers in patients with RTT. We have previously investigated the levels of various factors in the blood, plasma, and cerebrospinal fluid (CSF) of RTT patients, including biogenic amines, lactate, melatonin, pyruvate and other citric acid cycle intermediates, substance P, β-endorphin and other neuropeptides, and a neuromodulator of β-phenylethylamine. In addition, we have performed near-infrared spectroscopy of the cerebral cortices in patients with RTT and genetic studies of the methyl-CpG-binding protein 2 (MECP2) in these patients. Taken together, the multiple abnormalities we and other authors have revealed in the various neurotransmitters/neuromodulator systems explain the pervasive effects of Rett syndrome. We also discuss the possible role of plasma ghrelin and present the results of our mouse study of the MECP2-null mutation using ES cells. Finally, we consider the potential for future analyses using our recently developed iPS cell system and discuss the future perspectives for the treatment and management of this disease.
© 2010 The Japanese Society of Child Neurology. Published by Elsevier B.V. All rights reserved.

Keywords: Rett syndrome; Methyl-CpG-binding protein 2; Pathophysiology; Neurotransmitters; Neuromodulators; MECP2-null mutation mouse model

1. Introduction

Rett syndrome (RTT) is a neurodevelopmental disorder characterized by normal early psychomotor development followed by the loss of psychomotor and acquired purposeful hand skills and the onset of stereotyped movement of the hands and gait disturbance [1–4]. The gene was discovered in 1999 and the disease was found to be caused by a mutation of the methyl-CpG-binding protein 2 [5,6]. However, in many ways this clinically peculiar condition remains a mystery, with no clear correlations between the gene mutation and abnormal biological markers, neuropathology and/or unique clinical symptoms and signs [1–4,6].

RTT is unique among genetic, chromosomal and other developmental disorders because of its usually sporadic occurrence, extreme female gender bias, early normal development and subsequent developmental regression, autonomic dysfunction, stagnation in brain growth and distinctive neuropathology. MECP2 mutations lead to the RTT phenotype in females, and profound congenital encephalopathy in males [7]. Research needs to be directed toward clarifying the link between the MECP2 involvement and the alterations in biological, neurochem-

* Corresponding author. Address: Department of Pediatrics and Child Health, Kurume University School of Medicine, 67 Asahi-machi, Kurume City 830-0011, Japan. Tel.: +81 942 31 7565; fax: +81 942 38 1792.
E-mail address: tmatsu@med.kurume-u.ac.jp (T. Matsuishi).

0387-7604/$ - see front matter © 2010 The Japanese Society of Child Neurology. Published by Elsevier B.V. All rights reserved.
doi:10.1016/j.braindev.2010.12.007

ical, and neurotransmitter/receptor systems, as well as toward developing new therapeutic modalities.

2. Neurotransmitters and biological markers

2.1. Biogenic amines

Nomura and Segawa have suggested that hypoactivity or underdevelopment in the biogenic amines might account for the range of abnormalities found in RTT. Specifically, they suggested that the disease might be associated with impairments in noradrenalin, serotonin, and dopamine based on a series of clinical, electrophysiological and polysomnographic studies. They have proposed that the following points are important in considering the pathophysiology of RTT. First, the characteristic symptoms and signs appear in sequence within a specific age from infancy. The earliest and pathognomonic manifestations of RTT are the autistic tendency and the decreased rate in head growth [8,9]. Their report has led to a proliferation of studies on biogenic amines in the cerebrospinal fluid (CSF) of RTT patients, as well as immunohistochemical studies, receptor studies, and neuroimaging studies. Together, these investigations have suggested that various neurotransmitters, neuromodulators, neurotrophic factors and neuronal markers may be involved in RTT. Zoghbi et al. have reported significant reductions in the levels of homovanillic acid (HVA) and in 3-methoxy-4-hydroxy-phenylethylene glycol (MHPG) in the CSF of children with RTT [10]. However, Perry et al. reported no difference in these levels between RTT patients and controls [11]. Therefore, whether or not CSF biogenic amines are actually altered in RTT remains a matter of controversy. However, a recent report showed that HVA and 5-HIAA were decreased in RTT patients and the $MECP2^{null/y}$ mouse brain [12]. In another study, the biogenic amines dopamine, serotonin, and noradrenalin, and their respective metabolites HVA, 5-hydroxyindoleacetic acid, and MHPG, were measured in tissues from selected brain regions obtained at postmortem from four patients with RTT. A marked reduction in each of these substances was observed and these changes appeared to be age-related [13,14]. In addition, the endogenous levels of dopamine and its metabolites have been shown to be decreased throughout the neocortex and basal ganglia of patients with RTT [15]. Kitt et al. have reported a mild-to-moderate reduction in the number and cell size of the basal forebrain cholinergic neurons in RTT patients compared with controls, which might explain the impaired cognitive function and microcephalus [16].

2.2. β-Phenylethylamine

We have reported decreased β-phenylethylamine (PEA) levels in the CSF of patients with RTT [17]. PEA is an endogenous amine synthesized by decarboxylation of phenylalanine in the dopamine neurons of the nigrostriatal system, and plays an important role in both the dopaminergic and noradrenergic systems. We have also reported reduced levels of PEA in the CSF of patients with Parkinson's disease. The PEA level was also negatively correlated with the severity of the Parkinson's disease [18].

2.3. β-Endorphin, substance P, melatonin

Myer et al. [19] and Budden et al. [20] have reported elevated CSF β-endorphin in RTT. However, elevated β-endorphin was not found in the brain, suggesting that the alteration in β-endorphin may be a secondary change. We have reported that the level of substance P was markedly decreased in the CSF in patients with RTT, and this was considered to play a role in the features of autonomic dysfunction that occur in RTT, including constipation, small and cold feet, progressive limb muscle weakness and muscle atrophy [21]. Substance P is a neurotransmitter or neuromodulator in the peripheral as well as the central nervous system (CNS). Substance P activity is associated with dopaminergic neurons in the substantia nigra and the striatum, the central autonomic nuclei, the dorsal root ganglia, and the peripheral autonomic ganglia [22]. Hedner et al. reported that substance P acted on the respiratory control system by at least two different mechanisms: the bulbo-pontine time setting mechanism, and the inspiratory off-switch mechanism [23]. Deguchi et al. reported that the substance P immunoreactivity was significantly decreased in brain tissues, especially the solitary tract and nucleus, parvocellular and pontine reticular nuclei, and locus coeruleus, with less significant decreases in the substantia nigra, central gray matter of the midbrain, and other regions. Glial fibrillary acidic protein (GFAP)-positive astrocytes were increased in the areas in which SP immunoreactivity was decreased [24]. Neurotrophic effects of substance P on the hippocampal neurons have been reported [25]. Sleep disturbances such as screaming attacks, fragmented nighttime sleep, and excessive daytime sleeping are also common features in patients with RTT. These symptoms may be due to the decreased levels of melatonin, and in fact, such symptoms are ameliorated by exogenous melatonin treatment [26–28].

2.4. Neurotrophic factors and others

Nerve growth factor (NGF) is known to be a trophic factor, especially for the cholinergic neurons of the basal forebrain. NGF has been shown to be markedly decreased in the CSF of RTT patients, which may explain the decreased brain size [29]. Chen et al. [30] and Martinowich et al. [31] groups found that MECP2 binds selectively to brain-derived neurotrophic factor (BDNF) promoter and functions to regulate expression

of the BDNF gene. Overexpression of BDNF indeed extended the lifespan, restored locomotor activity levels, and relieved some symptoms of the MECP2 mutant phenotype [32,33]. Itoh et al. reported that MECP2 directly regulates expression of insulin-like growth factor binding protein 3 (IGFBP3) gene, which can be expected in turn to inhibit IGF-1 signaling [34,35].

Blue et al. reported significant changes in specific glutamate receptors, including NMDA, AMPA, and metabotropic type glutamate receptors in RTT [36]. Hamberger et al. have reported an elevation in the glutamate level in the CSF of children with RTT [37]. The elevations in NMDA receptors combined with the increased levels of CSF glutamate have suggested that excitatory neurotransmission is enhanced early in the course of the disease. Yamashita et al. measured benzodiazepine binding in stage IV RTT using single-photon computed tomography (SPECT) imaging techniques, and noted a significant reduction in the fronto-temporal cortex, suggesting a decrease in GABA receptors in adult RTT patients [38].

3. Energy metabolism: Rett syndrome is not a mitochondrial disease

Haas et al. have reported elevated CSF lactate and pyruvate in some patients with RTT [39]. Wakai et al. have reported morphological changes in the mitochondria in sural nerve biopsy specimens from patients with RTT [40]. We have also reported that the elevation in CSF lactate levels constituted a secondary biochemical change directly related to the abnormalities in respiration [41,42]. In a related study, we continuously monitored changes in cerebral oxygenation and hemodynamics in the frontal lobes of six patients with Rett syndrome during the awake state, which is associated with hyperventilation (HV) and breath-holding (BH), by near-infrared spectroscopy. We found that oxygenated hemoglobin (HbO_2) and total hemoglobin (HbT) decreased significantly during HV and BH in the awake state compared with the sleep state. The observed continuous decreases in HbO_2 and HbT may cause the focal ischemia and the increased lactate levels in the brain [43]. These finding suggested that RTT was not a primary mitochondrial disorder.

4. Neuropathological study

Armstrong reviewed the neuropathology of RTT and pointed out several important points as follows. The RTT brain is much smaller than a normal brain, and the volume is reduced in specific brain regions including the prefrontal, frontal, and anterior temporal regions. In addition, there are alterations of dendritic arborization in the above brain regions, and some Rett neurons have decreased expression of prealbumin and synaptophysin immunoreactivity and altered expression of neurotransmitters. Previous neuropathologic studies have also observed decreased melanin content of the zona compacta nigrae in the CNS of RTT patients [44]. Reduced expression of neuropeptides has been observed, including reduced immunoreactivity for tyrosine hydroxylase, a reduction of substance P in the parabrachial complex, and reductions of methionine enkephalin in the brainstem and the basal ganglia [45].

5. Methyl-CpG-binding protein 2 gene

Amir et al. reported on the clinical and laboratory features versus the genotype of MECP2. They also reported that the CSF HVA was significantly decreased in patients with truncating mutations compared with that in patients with missense mutations [46]. Methylation of DNA is essential for development in the mouse and plays an important role in the activation of the X-chromosome, genomic imprinting and gene silencing. The spectrum of MECP2 mutations reflects the importance of the methyl-CpG-binding domain and transcriptional repression domains [47]. Mutation analyses of the MECP2 gene have been performed in Japanese patients with RTT. The T158M mutation is a common mutation in the typical phenotype of RTT [48,49], while the R133C mutation was associated with the mildest cases with preserved speech [46,50]. We have already presented our preliminary clinical and basic research and reviewed the previous literature on RTT [51].

6. Future intervention and therapeutic strategies

6.1. Ghrelin

Ghrelin, a 28 amino acid peptide isolated from the rat stomach as an endogenous ligand for growth hormone secretagogue receptor (GHS-R) 1a and expressed in both the stomach and hypothalamus, exerts multiple physiological functions, including the stimulation of somatic growth, improvement of appetite, and enhancement of the motility of the gut [52]. Many of these functions are related to the clinical phenotypes of RTT, and thus this study investigated the plasma levels of ghrelin in 23 RTT patients in comparison to those in 39 healthy controls. The total ghrelin level in the patients with RTT was 127 ± 71 fmol/ml, and that in the controls was 228 ± 12 fmol/ml; the difference was statistically significant ($P < 0.01$). Thus ghrelin may play an important role in the pathophysiology of RTT.

6.2. MECP2-null mutation mouse model

In collaboration with Kosai et al. we developed an MECP2-null ES cell system using an adenoviral conditional targeting method [53]. We showed the roles of

MECP2 in neuronal development in terms of neuronal stem cells, neuronal and glial cell differentiation during all developmental stages, the function of differentiated dopaminergic neurons, and the maturation of neuronal cells. All these results should prove useful for understanding not only the biological roles of MECP2 but also the pathogenesis of RTT. Recently, we also developed an iPS cell system that may provide a novel strategy for developmental analysis at the molecular and cellular levels.

7. Conclusion

Finally, we should consider the potential for future mouse studies on MECP2-null mutation using ES cells and iPS cells and discuss the future perspectives for the treatment and management of this disease.

The reversal of early lethality and of some neurological abnormalities in MECP2-/Y mice through the postnatal supply of normal MECP2 has raised hopes for an effective treatment [54]. To this end, we should continue to explore new therapeutic modalities, including ghrelin, BDNF [32], and other factors [35].

Acknowledgements

This study was partly supported by a Grant on Research on Psychiatric and Neurological Diseases and Mental Health (#19-8), a Grant from the Research Project for Overcoming Intractable Diseases (#21-Nan-chi-ippan-110) and a Grant on Research on Learning Disorders (#19-6) from the Ministry of Health, Labour and Welfare of Japan, and was also partly supported by a Grant-in-Aid for Scientific Research C (#18591172) from the Ministry of Education, Culture, Sports, Science and Technology (MEXT) of Japan.

We are grateful to Drs. Ken-ichiro Kosai, Yasunori Okabe, Yoshihiro Nishi, Munetsugu Hara, Jyunko Yoh, and Yasuyuki Kojima for their contribution. Finally, we would like to acknowledge the patients and the family members of the Rett Syndrome Association (Sakuranbo-kai). This manuscript was presented as a presidential report of the 52nd Annual Meeting of the Japanese Society of Child Neurology (in Japanese) which had been held on May 20–22, 2010, Fukuoka Japan.

References

[1] The Rett Syndrome Diagnostic Criteria Work Group. Diagnostic criteria for Rett syndrome. Ann Neurol 1988;23:425–8.
[2] Kerr AM, Nomura Y, Armstrong D, Anvret M, Belichenko PV, Budden S, et al. Guidelines for reporting clinical features in cases with MECP2 mutations. Brain Dev 2001;23:208–11.
[3] Hagberg B, Hanefeld F, Percy A, Skjeldal O. An update clinically appreciable diagnostic criteria in Rett syndrome. Comments to Rett syndrome clinical criteria consensus panel satellite to European Pediatric Neurology Society Meeting, 11 September 2001, Germany: Baden Baden, Eur J Pediatr Neurol 2002; 6: 1–5.
[4] Chahrour M, Zoghbi HY. The story of Rett syndrome: from clinic to neurobiology. Neuron 2007;56:422–37.
[5] Amir RE, Van den Veyver IB, Wan M, Tran CQ, Francke U, Zoghbi HY. Rett syndrome is caused by mutations in X-linked MECP2, encoding methyl-CpG-binding protein 2. Nat Genet 1999;23:185–8.
[6] Bienvenu T, Chelly J. Molecular genetics of Rett syndrome: when DNA methylation goes unrecognized. Nat Rev Genet 2006;7:415–26.
[7] Franke U. Rett syndrome and MECP2-status of knowledge 10 years after the genes. Invited speaker of Segawa program. No to Hattatsu 2010;42:S88.
[8] Nomura Y, Honda K, Segawa M. Pathophysiology of Rett syndrome. Brain Dev 1987;9:506–13.
[9] Segawa M, Nomura Y. Polysomnography in the Rett syndrome. Brain Dev 1992;14:S46–54.
[10] Zoghbi H, Milstien H, Butler IJ, Smith OB, Kaufman S, Glaze DG, et al. Cerebrospinal fluid biogenic amines and biopterin in Rett syndrome. Ann Neurol 1989;25:56–60.
[11] Perry TL, Dunn HG, Ho H-H, Crichton JU. Cerebrospinal fluid values for monoamine metabolites, gamma aminobutyric acid, and other amino compounds in Rett syndrome. J Pediatr 1988;112:234–8.
[12] Samaco RC, Mandel-Brehm C, Chao H-T, Ward CS, Fyffe-Maricich SL, Ren J, et al. Loss of MeCP2 in aminergic neurons causes cell-autonomous defects in neurotransmitter synthesis and specific behavioral abnormalities. PNAS 2009;106:21966–71.
[13] Lekman A, Witt-Engerstrom I, Gottfries J, Hagberg B, Percy AK, Svennerholm L. Rett syndrome: biogenic amines and metabolites in postmortem brain. Pediatr Neurol 1989;5:357–62.
[14] Ide S, Itoh M, Goto Y. Defect in normal developmental increase of the brain biogenic amine concentrations in the mecp2-null mouse. Neurosci Lett 2005;386:14–7.
[15] Wenk GL. Alteration in dopaminergic function in Rett syndrome. Neuropediatrics 1995;26:123–5.
[16] Kitt CA, Troncoso JC, Price DL, Naidu S, Moser H. Pathological changes in substantia nigra and basal forebrain neurons in Rett syndrome. Ann Neurol 1990;28:416–7.
[17] Satoi M, Matsuishi T, Yamada S, Yamashita Y, Ohtaki E, Mori K, et al. Decreased cerebrospinal fluid levels of β-phenylethylamine in patients with Rett syndrome. Ann Neurol 2000;47:801–3.
[18] Zhou G, Shoji H, Yamada S, Matsuishi T. Decreased cerebrospinal fluid β-phenylethylamine in Parkinson's disease. J Neurol Neurosurg Psychiatry 1997;63:754–8.
[19] Myer EC, Tripathi HL, Dewey WL. Hyperendorphinism in Rett syndrome: cause or result? Ann Neurol 1988;24:340–1.
[20] Budden SS, Myer EC, Buttler IJ. Cerebrospinal fluid studies in the Rett syndrome: biogenic amines and beta endorphins. Brain Dev 1990;12:81–4.
[21] Matsuishi T, Nagamitsu S, Yamashita Y, Murakami Y, Kimura A, Sakai T, et al. Decreased cerebrospinal fluid levels of substance P in patients with Rett syndrome. Ann Neurol 1997;42:978–81.
[22] Mai JK, Stephens PH, Hope A, Cuello AC. Substance P in the human brain. Neuroscience 1986;17:709–39.
[23] Hender J, Hender T, Wessberg P, Jonason J. Interaction of substance P with respiratory control system in the rat. J Pharmacol Exp Ther 1983;228:196–201.
[24] Deguchi K, Antalffy BA, Twohill LJ, Chakraborty S, Glaze DG, Armstrong DD. Substance P immunoreactivity in Rett syndrome. Pediatr Neurol 2000;22:259–66.
[25] Whitty CJ, Kapatos G, Bannon MJ. Neurotrophic effects of substance P on hippocampal neurons in vitro. Neurosci Lett 1993;164:141–4.

[26] McArthur AJ, Budden SS. Sleep dysfunction in Rett syndrome: a trial of exogenous melatonin treatment. Dev Med Child Neurol 1998;40:186–92.
[27] Miyamoto A, Oki J, Takahashi S, Okuno A. Serum melatonin kinetics and long-term melatonin treatment for sleep disturbance in Rett syndrome. Brain Dev 1999;21:59–62.
[28] Yamashita Y, Matsuishi T, Murakami Y, Kato H. Sleep disorder in Rett syndrome and melatonin treatment. Brain Dev 1999;21:570.
[29] Lappalainen R, Lindholm D, Riikonen R. Low levels of nerve growth factor in cerebrospinal fluid of children with Rett syndrome. J Child Neurol 1996;11:296–300.
[30] Chen WG, Chang Q, Lin Y, Meissner A, West AE, Griffith EC, et al. Derepression of BDNF transcription involves calcium-dependent phosphorylation of MeCP2. Science 2003;302:885–9.
[31] Martinowich K, Hattori D, Wu H, Fouse S, He F, Hu Y, et al. DNA methylation-related chromatin remodeling in activity-dependent BDNF gene regulation. Science 2003;302:890–3.
[32] Chang Q, Khare G, Dani V, Nelson S, Jaenisch R. The disease progression of Mecp2 mutant mice is affected by the level of BDNF expression. Neuron 2006;49:341–8.
[33] Larimore JL, Chapleau CA, Kudo S, Theibert A, Percy AK, Pozzo-Miller L. Bdnf overexpression in hippocampal neurons prevents dendritic atrophy caused by Rett-associated MECP2 mutations. Neurobiol Dis 2009;34:199–211.
[34] Itoh M, Ide S, Takashima S, Kudo S, Nomura Y, Segawa M, et al. Methyl CpG-binding protein 2 (a mutation of which causes Rett syndrome) directly regulates insulin-like growth factor binding protein 3 in mouse and human brains. J Neuropathol Exp Neurol 2007;66:117–23.
[35] Tropea D, Giacometti E, Wilson NR, Beard C, McCurry C, Fu DD, et al. Partial reversal of Rett syndrome-like symptoms in MeCP2 mutant mice. Proc Natl Acad Sci USA 2009;106:2029–34.
[36] Blue ME, Naidu S, Johnston MV. Development of amino acid receptors in frontal cortex from girls with Rett syndrome. Ann Neurol 1999;45:541–5.
[37] Hamberger A, Gillberg C, Palm A, Hagberg B. Elevated CSF glutamate in Rett syndrome. Neuropediatrics 1992;23:212–3.
[38] Yamashita Y, Matsuishi T, Ishibashi M, Kimura A, Onishi Y, Yonekura Y, et al. Decrease in benzodiazepine receptor binding in the brain of adult Rett syndrome. J Neurol Sci 1998;154:146–50.
[39] Haas RH, Rice MA, Trauner DA, Meritt A. Ketogenic diet in Rett syndrome. Am J Med Genet 1986;24(Suppl 1):5225–46.
[40] Wakai S, Kameda K, Ishikawa YI, Miyamoto S, Nagaoka M, Okabe M, et al. Rett syndrome: findings suggesting axonopathy and mitochondrial abnormalities. Pediatr Neurol 1990;6:164–6.
[41] Matsuishi T, Urabe F, Komori H, Yamashita Y, Naito E, Kuroda Y, et al. The Rett syndrome and CSF lactic patterns. Brain Dev 1992;14:68–70.
[42] Matsuishi T, Urabe F, Percy AK, Komori H, Yamashita Y, Schultz RS, et al. Kato H Abnormal carbohydrate metabolism in cerebrospinal fluid in Rett syndrome. J Child Neurol 1994;9: 26–30.
[43] Murakami Y, Yamashita Y, Matsuish T, Iwanaga R, Kato H. Cerebral oxygenation and hemodynamics during hyperventilation and sleep in patients with Rett syndrome. Brain Dev; 20: 574–578.
[44] Armstrong DD. Rett syndrome neuropathology review 2000. Brain Dev 2001;23:S72–6.
[45] Saito Y, Ito M, Ozawa Y, Matsuishi T, Hamano K, Takashima S. Reduced expression of neuropeptides can be related to respiratory disturbances in Rett syndrome. Brain Dev 2001;23:S122–6.
[46] Amir RE, Van den Veyver IB, Schultz R, Malicki DM, Tran CQ, Dahle EJ, et al. Influence of mutation type and X chromosome inactivation on Rett syndrome phenotypes. Ann Neurol 2000;47:670–9.
[47] Nan X, Bird A. The biological function of the methyl-CpG binding protein MECP2 and its implication in Rett syndrome. Brain Dev 2001;23:S32–7.
[48] Obata K, Matsuishi T, Yamashita Y, Fukuda T, Kuwajima K, Horiuchi I, et al. Mutation analysis of the Methyl-CpG binding protein 2 gene (MECP2) in patients with Rett syndrome. J Med Genet 2000;37:608–10.
[49] Fukuda T, Yamashita Y, Nagamitsu S, Miyamoto K, Jin JJ, Ohmori I, et al. Methyl-CpG binding protein 2 gene (MECP2) variations in Japanese patients with Rett syndrome: pathological mutations and polymorphisms. Brain Dev 2005;27:211–7.
[50] Yamashita Y, Kondo I, Fukuda T, Morishima R, Kusaga A, Iwanaga R, et al. Mutation analysis of the methyl-CpG-binding protein 2 gene (MECP2) in Rett patients with preserved speech. Brain Dev 2001;23:S157–60.
[51] Matsuishi T, Yamashita Y, Kusaga A. Neurobiology and neurochemistry of Rett syndrome. Brain Dev 2001;23:S58–61.
[52] Yoshihara F, Kojima M, Hosoda H, Nakazato M, Kangawa K. Ghrelin: a novel peptide for growth hormone release and feeding regulation. Curr Opin Nutr Metab Care 2002;5:391–5.
[53] Okabe Y, Kusaga A, Takahashi T, Mitsumasu C, Murai Y, Tanaka E, et al. Neural development of methyl-CpG-Binding protein 2-null embryonic stem cells: a system for studying Rett syndrome. Brain Res 2010 in press.
[54] Guy J, Gan J, Selfridge J, Cobb S, Bird A. Reversal of neurological defects in a mouse model of Rett syndrome. Science 2007;315:1143–7.

Human Molecular Genetics, 2011, Vol. 20, No. 19 **3798–3810**
doi:10.1093/hmg/ddr298
Advance Access published on July 1, 2011

Neuron-specific impairment of inter-chromosomal pairing and transcription in a novel model of human 15q-duplication syndrome

Makiko Meguro-Horike[1], Dag H. Yasui[2], Weston Powell[2], Diane I. Schroeder[2], Mitsuo Oshimura[3], Janine M. LaSalle[2] and Shin-ichi Horike[1,*]

[1]Frontier Science Organization, Kanazawa University, 13-1 Takaramachi, Kanazawa 920-0934, Japan, [2]Department of Medical Microbiology and Immunology, Genome Center and M.I.N.D. Institute, University of California Davis School of Medicine, 1 Shields Avenue Davis, CA 95616, USA and [3]Department of Biomedical Science, Tottori University, 86 Nishi-cho, Yonago, Tottori 683-8503, Japan

Received April 3, 2011; Revised June 25, 2011; Accepted June 28, 2011

Although the etiology of autism remains largely unknown, cytogenetic and genetic studies have implicated maternal copy number gains of 15q11–q13 in 1–3% of autism cases. In order to understand how maternal 15q duplication leads to dysregulation of gene expression and altered chromatin interactions, we used microcell-mediated chromosome transfer to generate a novel maternal 15q duplication model in a human neuronal cell line. Our 15q duplication neuronal model revealed that by quantitative RT–PCR, transcript levels of *NDN*, *SNRPN*, *GABRB3* and *CHRNA7* were reduced compared with expected levels despite having no detectable alteration in promoter DNA methylation. Since 15q11–q13 alleles have been previously shown to exhibit homologous pairing in mature human neurons, we assessed homologous pairing of 15q11–q13 by fluorescence *in situ* hybridization. Homologous pairing of 15q11–q13 was significantly disrupted by 15q duplication. To further understand the extent and mechanism of 15q11–q13 homologous pairing, we mapped the minimal region of homologous pairing to a ~500 kb region at the 3′ end of *GABRB3* which contains multiple binding sites for chromatin regulators MeCP2 and CTCF. Both active transcription and the chromatin factors MeCP2 and CTCF are required for the homologous pairing of 15q11–q13 during neuronal maturational differentiation. These data support a model where 15q11–q13 genes are regulated epigenetically at the level of both inter- and intra-chromosomal associations and that chromosome imbalance disrupts the epigenetic regulation of genes in 15q11–q13.

INTRODUCTION

Autism spectrum disorders (ASDs; MIM 209850) include a complex group of neurodevelopmental disorders characterized by impairments in reciprocal social interactions, problems in communication and a restricted range of behaviors and interests. ASD affects individuals of all socio-economic and cultural backgrounds and has a prevalence of 6 per 1000 individuals, with males affected four times more frequently than females (1,2). There is compelling evidence for a genetic etiology of ASD from twin studies that have shown high concordance between monozygotic twins (3–5). To date, cytogenetic studies have identified a number of pathogenic chromosomal anomalies in ASD patients (1). In addition, current microarray-based technologies have enabled the detection of submicroscopic microdeletions and microduplications [copy number variations (CNVs)] and revealed that submicroscopic CNVs can have a pathogenic role in ASD as well (3,4). Human chromosome 15q11–q13 is frequently involved in clinically important genomic rearrangements, including interstitial deletions, duplications and supernumerary marker chromosome, called isodicentric chromosome (idic) (5). After fragile X, maternal 15q11–q13 duplications are the most common cytogenetic cause of autism, occurring in ~1–3% of individuals with ASD (6–9). A recent analysis of 10K single-nucleotide polymorphism data identified 15q11–q13 CNVs in 17 of 1749 autism patients (10).

*To whom correspondence should be addressed. Tel: +81 762652775; Fax: +81 762344537; Email: sihorike@staff.kanazawa-u.ac.jp

© *The Author 2011. Published by Oxford University Press. All rights reserved.*
For Permissions, please email: journals.permissions@oup.com

Genomic imprinting is an epigenetic mechanism that establishes parent-of-origin-specific gene expression patterns. Deletions of 15q11–q13 on the paternal chromosome 15 cause Prader–Willi syndrome (PWS; MIM 176270), whereas maternal deletions cause Angelman syndrome (AS; MIM 105830) (11). Parental differences in DNA methylation at imprinting control regions have a crucial role in genomic imprinting of 15q11–q13, as well as differences in DNA replication timing, histone modifications, chromosome nuclear organization and mitotic recombination frequencies (12). However, despite progress in molecular characterization of 15q11–q13 rearrangements and imprinting mechanisms, the molecular pathogenesis of the autism phenotype resulting from maternal 15q11–q13 duplications remains largely unknown. The ubiquitin E3 ligase gene *UBE3A* is the primary candidate gene presumed to be dysregulated in 15q duplication syndrome because of imprinted maternal expression in the brain. In particular, *UBE3A* has been analyzed due to its role in AS, its pattern of imprinting and its biological function (13–15). However, 15q11–q13 duplications also include the cluster of three gamma-aminobutyric acid A receptor ($GABA_AR$) subunit genes (*GABRB3, GABRA5, GABRG3*) and paternally expressed genes implicated in splicing (*SNRPN*), circadian rhythm (*MAGEL2*), respiration (*NDN*) and nucleolar function (*HBII85, HBII52*) (16,17). While increased copy number of 15q11–q13 was predicted to increase expression of the maternally expressed *UBE3A* and biallelically expressed genes such as *GABRB3* and *GABRA5*, prior investigation of an idic15 brain sample with PWS-like features instead showed reduced levels of *GABRB3*, *GABRA5*, *GABRG3*, *SNRPN*, *HBII85* and *HBII52* (18). The striking parent-of-origin pattern of inheritance for 15q11–q13 rearrangements has led to the hypothesis that higher order epigenetic dysregulation of transcription within this region may be involved in ASD.

The higher order, inter-chromosomal association of homologous pairing of maternal and paternal alleles of 15q11–q13 was originally described in lymphocytes and predicted to regulate maintenance of imprinting in the locus (19). Homologous pairing of 15q11–q13 was shown to occur in neurons and be deficient in brains of individuals with Rett syndrome (RTT; MIM 312750), autism and maternal 15q duplication (18,20). Although these observations raise the possibility that homologous pairing of 15q11–q13 is an important spatial organization modulating neuron-specific transcripts within the paired regions, the mechanisms of homologous pairing and its effects on gene expression within the paired regions in neurons has not been previously determined.

Here, we made use of microcell-mediated chromosome transfer (MMCT) technology to generate a 15q11–q13 maternal duplication model in a human neuronal cell line. Using this MMCT method, a maternal copy of human chromosome 15 was successfully transferred into human SH-SY5Y neuronal cells. Our experimental models of 15q duplication syndrome recapitulated the reduced levels of several transcripts resulting from increased maternal 15q11–q13 dosage previously observed in the brain as well as the reduced homologous pairing. We further show that the chromatin regulators MeCP2 and CTCF are required for the homologous pairing of 15q11–q13 during neuronal differentiation. These results provide insight into the inter- and intra-chromosomal spatial interactions influencing 15q11–q13 transcript levels in neurons and provide support for an epigenetic dysregulation pathway by which 15q11–q13 duplications may result in ASD.

RESULTS

Establishment of a maternal 15q duplication model by microcell fusion

We have previously established mouse A9 hybrid cells retaining a single human chromosome of defined parental origin for the investigation of imprinted loci in humans (21). Gene expression and DNA methylation studies demonstrated that the appropriate imprinting status of human loci was maintained in mouse A9 hybrids (22–24). In this study, to generate a novel maternal 15q duplication model in a neuronal cell line, a maternal human chromosome 15 was transferred from mouse A9 hybrids into human SH-SY5Y neuronal cells by MMCT (Fig. 1A). SH-SY5Y cells were selected as a recipient cell line because they can be induced to undergo differentiation within 72 h using PMA, resulting in a morphologic change in the extension of axonal projections and the increased expression of neuron-specific enolase (25). In addition, SH-SY5Y cells are diploid for most chromosomes (26). Our PCR-restriction fragment length polymorphism (RFLP) analysis identified 20 independent SH-SY5Y microcell hybrids that contained an extra maternal copy of human chromosome 15, and therefore named SH(15M) cell lines (Fig. 1B). To further confirm the state of the introduced maternal human chromosome 15 in SH-SY5Y cells, we performed cytogenetic analyses using fluorescence *in situ* hybridization (FISH) (Fig. 1C). Finally, we confirmed that introduced maternal chromosome 15 was maintained stably in SH(15M) cell lines under appropriate selection conditions. For further analyses, we selected three independent SH(15M) cell lines that morphologically resembled parental SH-SY5Y cells.

Quantitation of 15q11–q13 transcripts in a maternal 15q duplication model

To determine the effect of increased maternal chromosome 15 dosage on transcript levels in SH(15M) cells, quantitative RT–PCR was used to measure the levels of eight transcripts at the 15q11–q13 locus and two non-15q11–q13 housekeeping gene controls, *GAPDH* and *ACTB* (Fig. 2A). The non-imprinted genes *CYFIP1* and *TJP1* revealed the expected 1.5-fold increase in transcript abundance in all three SH(15M) cell lines (Fig. 2B and C). In contrast, expression of non-imprinted *GABRB3* and *CHRNA7* genes was significantly reduced compared with the parental cell line in all three SH(15M) lines, despite increased 15q11–q13 dosage (Fig. 2D and E). Moreover, paternal expression of *NDN* and *SNRPN* transcripts was also significantly reduced despite the increased maternal dosage (Fig. 2F and G). Furthermore, there was no difference between control SH-SY5Y cells and SH(15M) cells in the levels of maternally expressed *UBE3A* transcript, even though a 2-fold increase was expected

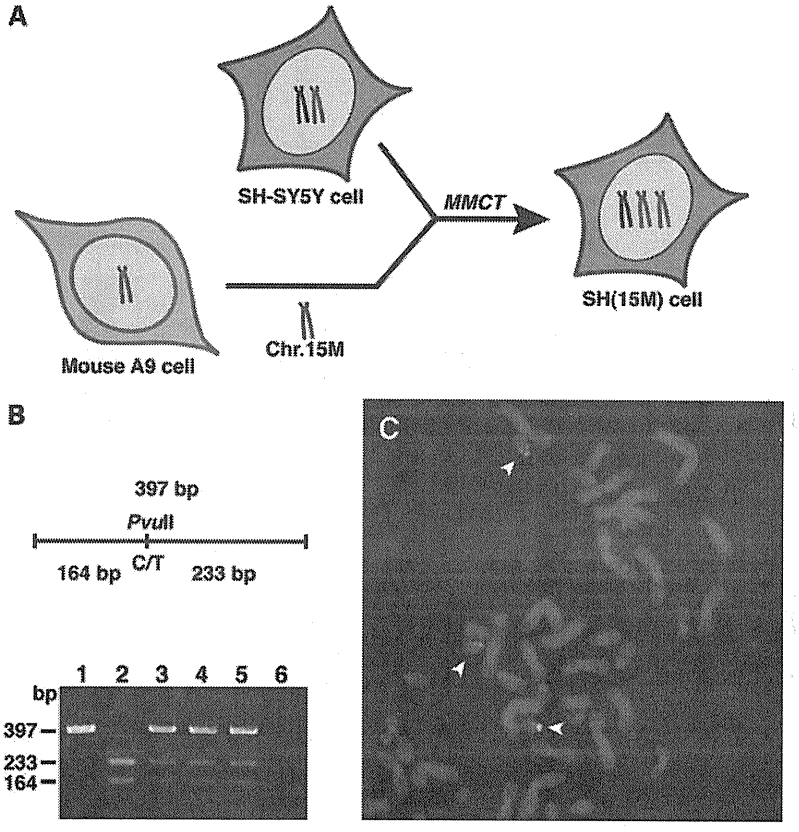

Figure 1. Characterization of SH-SY5Y neuronal cells containing an extra maternal human chromosome 15. (**A**) A schematic diagram showing the construction of SH-SY5Y microcell hybrids [SH(15M) cell] containing an extra maternal copy of human chromosome 15. Transfer of a maternal human chromosome 15 from mouse A9 cells to SH-SY5Y cell was performed by MMCT technology. (**B**) RFLP analysis to confirm presence of donor chromosome 15 in SH(15M) cells is shown. DNA from introduced maternal human chromosome 15 donor A9 cells (lane 1), SH-SY5Y cells (lane 2), SH(15M)-1, 2, 3 cells (lanes 3–5) and mouse A9 cells (lane 6) was amplified by PCR using primers that span a *Pvu*II polymorphism. Both chromosome 15 copies in the host SH-SY5Y cells were digested by *Pvu*II, but the donor chromosome 15 was undigested. SH(15M) cells contained both digested and undigested fragments. (**C**) Results from DNA-FISH analysis of SH(15M) cells. Metaphase chromosomes from SH(15M) were hybridized *in situ* with Vysis LSI *GABRB3* (red) and CEP15 (green) probes. The arrowheads indicate three copies of chromosome 15.

(Fig. 2H). In addition, another maternally expressed gene, *ATP10A*, was also significantly reduced despite the increased maternal dosage (Fig. 2I). While extra copies of genes are expected to result in increased transcript levels, our SH(15M) cell lines recapitulated the direction of transcriptional alterations previously observed in a human brain sample with maternal 15q duplication (18).

We next assessed the DNA methylation status of *NDN, SNRPN, UBE3A, GABRB3* and *CHRNA7* promoter CpG islands by bisulfite sequencing to determine whether the DNA methylation status of these promoters was correlated with the observed reductions in transcript levels. *GABRB3, CHRNA7* and *UBE3A* promoters in the SH(15M) cells were almost completely unmethylated and appeared similar to those observed in control SH-SY5Y cells (Supplementary Material, Fig. S1A–C). Similarly, the expected maternal DNA methylation levels were observed for *NDN* and *SNRPN* promoter CpG islands in both SH-SY5Y cells and SH(15M) cells (Supplementary Material, Fig. S1D and E). Because these CpG islands are differentially methylated in a parent-of-origin-specific manner, increased DNA methylation levels were expected following chromosome transfer of the methylated maternal allele (27,28). A combined bisulfite restriction analysis (29) showed strong concordance with bisulfite sequencing results (data not shown). These findings indicate that promoter DNA methylation is not correlated with altered transcript levels of *NDN, SNRPN, UBE3A, GABRB3* or *CHRNA7* in SH(15M) cells.

Disruption of 15q11–q13 homologous pairing in a maternal 15q duplication model

Homologous chromosomal association or pairing of maternal and paternal 15q11–q13 alleles has previously been described in both lymphocytes (19) and neurons (20) and disrupted in the 15q dup brain (18). Therefore, we investigated the impact of an extra maternal human chromosome 15 on normal interactions between maternal and paternal 15q11–q13 alleles. In comparison with SH-SY5Y cells, SH(15M) cells displayed a significant reduction in the percentage of paired alleles for nuclei hybridized with a Vysis LSI *GABRB3* probe (Fig. 3A and B). However, there was no difference in the percentage of paired alleles of nuclei hybridized with a control chromosome 15 pericentromeric CEP15 probe. Homologous pairing was

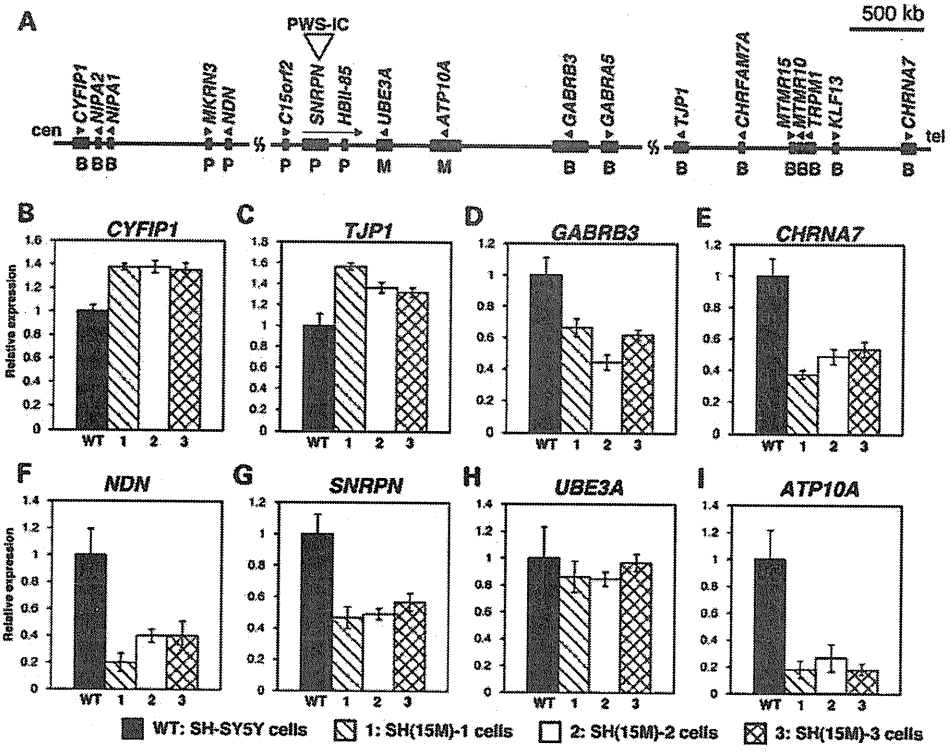

Figure 2. Analysis of 15q11–q13 transcript levels in experimental model of dup15q syndrome. (**A**) Physical map of the imprinted gene cluster in human chromosome 15q11–q13. PWS-IC is the PWS imprinting center, which is essential for establishment of the paternal epigenetic state of the region. Genes or transcripts (filled boxes) are drawn approximately to scale. Transcriptional direction is indicated by arrowheads and arrows. P, paternally expressed genes; M, maternally expressed genes; B, biallelically expressed genes. (**B–I**) Summary of quantitative RT–PCR measurements of eight transcripts in 15q11–q13, normalized to the housekeeping genes *GAPDH* and *ACTB*. Error bars represent ± SEM. All qRT–PCR analyses were performed on cDNA from PMA-treated differentiated SH-SY5Y cells (WT) and PMA-treated differentiated SH(15M) cells (1–3). (B)–(E) are non-imprinted biallelically expressed genes, (F) and (G) are paternally expressed imprinted genes and (H) and (I) are maternally expressed imprinted genes.

not observed in either SH-SY5Y or SH(15M) cells hybridized with a non-15 control, a pericentromeric probe specific for chromosome 11 (CEP11; data not shown). Thus, the extra maternal human chromosome 15 in the SH(15M) cells conferred a specific effect on the nuclear organization of 15q11–q13 and modeled the homologous pairing defect previously observed in the 15q duplication syndrome brain (18). In addition, our observations indicate that homologous pairing of 15q11–q13 could influence gene expression within the paired region.

Homologous pairing of 15q11–q13 in the 3′ region of the *GABRB3* gene

The mechanism of homologous pairing of 15q11–q13 in neurons is poorly understood, but critical for understanding the changes in transcription that accompany the loss of homologous pairing in 15q duplication syndrome. To map the precise location and extent of 15q11–q13 homologous pairing upon neuronal differentiation, we performed additional FISH analyses using nine different fluorescently labeled bacterial artificial chromosome (BAC) probes distributed over 9 Mb of 15q11–q13 (Fig. 4A). We measured the inter-chromosomal distances between FISH signals from each BAC probe both before (untreated) and 72 h after differentiation with PMA (PMA treated) (20). In comparison with undifferentiated SH-SY5Y cells, a high percentage of nuclei displayed close inter-chromosomal distances (2 μm or less) at the *GABRB3* locus following neuronal differentiation, as shown by a significant leftward shift in the distribution (Fig. 4B–E). In contrast to the significant decrease observed in inter-chromosome distances at *GABRB3*, the *CYFIP* locus showed the opposite pattern, with a significant increase in inter-chromosome distance following differentiation (Fig. 4B–D).

To narrow down the genomic region in which the homologous inter-chromosomal association was observed, we performed detailed frequency analyses of homologous allele distances across the $GABA_AR$ subunit gene cluster (Fig. 5A). Homologous pairing of 15q11–q13 was observed in the 3′ region of the *GABRB3* gene, but not in *GABRA5* and *GABRG3* (Fig. 5B–D). This in-depth analysis of multiple FISH probes therefore narrowed the locus of homologous interaction to a ~500 kb region at the 3′ end of *GABRB3*, with significant changes in homologous pairing during SH-SY5Y differentiation limited to the region detected by a single BAC probe, GABRB3(2).

Because clustering of *$GABA_AR$* subunit genes is well conserved on human chromosomes 4, 5, 15 and X, it has previously been hypothesized that the physical proximity of $GABA_AR$ subunit genes facilitates temporally and spatially coordinated expression (30). Therefore, we wished to test whether the homologous chromosomal association is also conserved in other clusters of *$GABA_AR$* subunit genes. To this end, the homologous

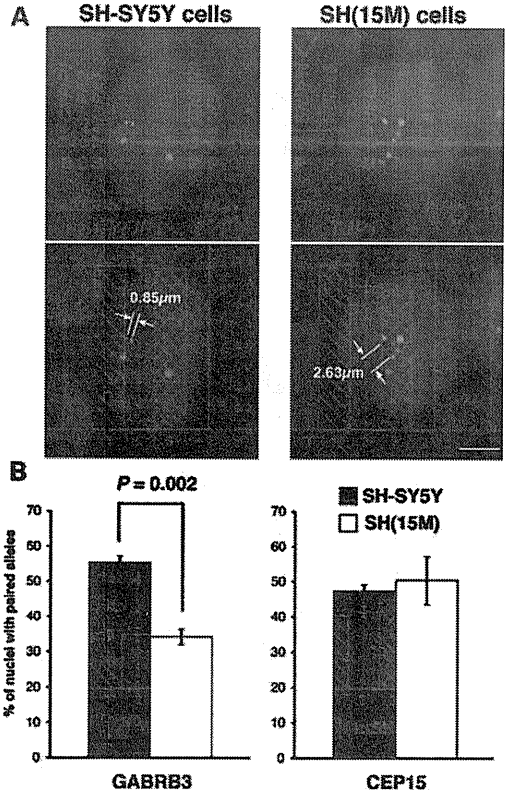

Figure 3. Reduced homologous pairing of *GABRB3* alleles as a result of duplicated maternal chromosome 15 in SH-SY5Y cells. (**A**) Representative image of chr.15–chr.15 localization in SH-SY5Y cells (left panel) and SH(15M) cells (right panel) using Vysis LSI *GABRB3* SpectrumOrange/CEP15 SpectrumGreen. The iVision software was used to measure distances between two signals. In case of SH(15M) cells, we measured the shortest interchromosomal distances between the three signals. Scale bars: 5 μm. (**B**) Differences in homologous pairing in SH-SY5Y cells (gray bars) and SH(15M) cells (white bars), as determined by hybridization with Vysis LSI *GABRB3* (left panel) and CEP15 (right panel) FISH probes. Pairing was scored as homologous FISH signals with distances ≤2 μm apart. The bars indicate the mean ± SEM of three replicate experiments, in each of which 100–150 nuclei were scored. Significantly fewer SH(15M) cell nuclei showed pairing when the *GABRB3* probe was used. In contrast, no significant difference was observed in SH(15M) cells in pairing between alleles detected by the pericentromeric CEP15 probe.

pairing analyses were extended to $GABA_AR$ subunit genes on 4p12 and 5q34 (Supplementary Material, Fig. S2). Unlike 15q11–q13, homologous pairings of 4p12 and 5q34 were not observed during neuronal differentiation. However, transcript levels for *GABRG1* and *GABRA4* on 4p12, and *GABRG2* and *GABRA6* on 5q34 were barely detectable in differentiated SH-SY5Y cells (data not shown). Cumulatively, our findings suggest that homologous chromosomal pairing in 15q11–q13 coincides with increased expression of $GABA_AR$ subunit genes specifically in this locus during neuronal differentiation, as *GABRB3* is highly expressed in differentiated SH-SY5Y cells (data not shown). Therefore, in order to investigate whether active transcription is necessary for homologous chromosomal pairing in 15q11–q13, differentiated SH-SY5Y cells were treated with the transcriptional inhibitor α-amanitin. The observation that α-amanitin caused significant decreases in the percentage of paired alleles for nuclei hybridized with *GABRB3* probe suggests that active transcription was required for homologous chromosomal pairing in 15q11–q13 (Fig. 4F).

Involvement of chromatin proteins MeCP2 and CTCF in regulation of 15q11–q13 homologous pairing

Our observations raise the question as to which factors control the homologous pairing of 15q11–q13. Notably, we observed multiple binding sites for MeCP2 and CTCF in a ~500 kb region between at the 3′ end of *GABRB3*. We used a short-interfering RNA (siRNA)-mediated knockdown approach to directly test the role of MeCP2 in the homologous pairing of 15q11–q13 by transiently depleting MeCP2 expression. MeCP2 protein depletion in differentiated SH-SY5Y cells was confirmed by western blot analysis and immunostaining (Fig. 6A–C) and chr.15–chr.15 interchromosomal distances were measured between FISH signals of GABRB3 and CEP15 probes (Fig. 6D). Consistent with previous findings, homologous pairing at *GABRB3* was significantly reduced in MeCP2 knockdown cells compared with non-targeting siRNA-treated cells (20). Specifically, the two GABRB3 FISH signals were ≤2 μm apart in only 18.5% of MeCP2-deficient nuclei compared with 48.9% in control cells.

CTCF is also required for inter- and intra-chromosomal associations during genomic imprinting and X inactivation (31–34). A chromatin immunoprecipitation assay using a CTCF-specific antibody demonstrated that there are three CTCF-binding sites at the 3′ region of the *GABRB3* gene (Supplementary Material, Fig. S3). Therefore, we examined whether CTCF deficiency affected homologous pairing at the *GABRB3* locus in differentiated SH-SY5Y cells. Western blot and immunostaining analyses showed that CTCF was predominantly depleted at the protein level (Fig. 6E–G). Interestingly, depletion of CTCF resulted in a significant reduction in the homologous pairing at *GABRB3*, and at CEP15 (Fig. 6H). In contrast, knocking down RAD21 had no obvious effect on the homologous pairing of 15q11–q13 (Supplementary Material, Fig. S4), although this protein has been reported to frequently accumulate at CTCF-binding sites (35). These results suggest that MeCP2 and CTCF are essential mediators for the homologous pairing of 15q11–q13.

DISCUSSION

Autism has been linked to the region on chromosome 15q11–q13 that is responsible for the imprinting disorders PWS and AS (1,3,5). Maternal 15q11–q13 duplications are the most frequent cytogenetically detectable mutation associated with ASD (6–9), but the molecular impact of 15q duplication in neurons has been difficult to assess because of the lack of an appropriate model system. While overexpression of maternally expressed *UBE3A* was predicted to be the major cause of the ASD phenotype in 15q duplication syndrome (36), Hogart and LaSalle (18) revealed that 15q11–q13 transcripts in maternal 15q11–q13 duplication brain samples were altered in a direction not predicted from maternal copy number gains. This led to the suggestion that an imbalance of 15q11–q13 dosage can disrupt normal epigenetic pathways such as parental homologous pairing and DNA methylation status, changing gene

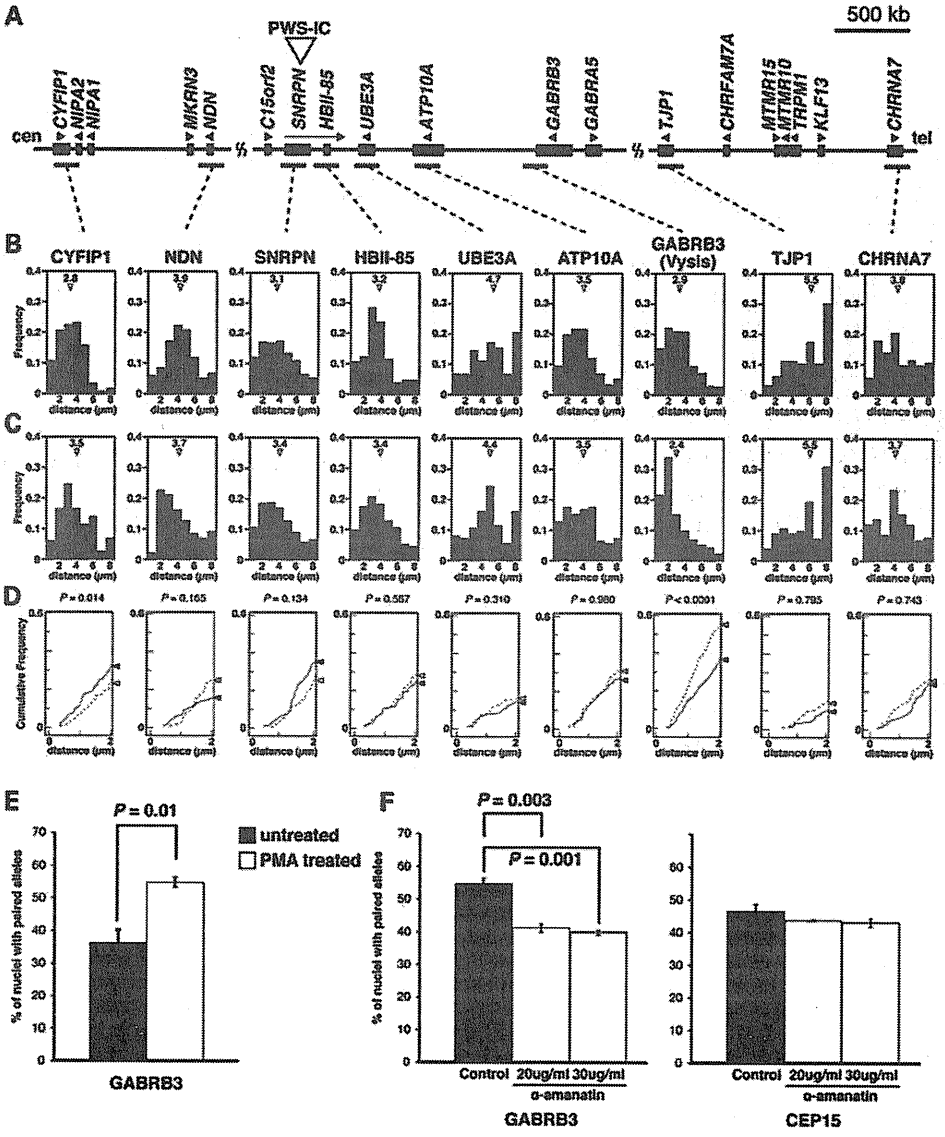

Figure 4. Increased homologous pairing of *GABRB3* alleles during neuronal differentiation is associated with active transcription. (**A**) Physical map of the imprinted gene cluster in human chromosome 15q11–q13. PWS-IC is the PWS imprinting center, which is essential for establishment of the paternal epigenetic state of the region. Genes or transcripts (filled boxes) are drawn approximately to scale. Transcriptional direction is indicated by arrowheads and arrows. The horizontal bars indicate BAC probes used in the pairing analyses. *GABRB3*(1) probe indicates the Vysis LSI *GABRB3* Spectrum Orange probe. (**B**) Frequency distribution of distances between homologous alleles at multiple sites along 15q11–q13 for undifferentiated SH-SY5Y cell nuclei, as measured on each BAC probe. Mean distance, open triangle. (**C**) Frequency distribution of distances between homologous alleles at multiple sites along 15q11–q13 for PMA-treated differentiated SH-SY5Y cell nuclei. Mean distance, open triangle. A high proportion of PMA-treated differentiated SH-SY5Y cells displayed close homologous distances ($\leq$2 μm) at *GABRB3* upon neuronal differentiation, as shown by a leftward shift in the distribution. (**D**) Cumulative distribution of distances between homologous alleles at 0–2 μm. The solid line indicates the undifferentiated SH-SY5Y cells. The dotted line indicates the PMA-treated differentiated SH-SY5Y cells. The closed and open triangles indicate cumulative frequency at 2 μm, respectively. The statistical relevance was assessed by a comparison of the entire histogram of measurement distributions from (B) and (C) using two non-parametric tests, namely Mann–Whitney's *U*-test and Kolmogorov–Smirnov test. *P*-values from Mann–Whitney's *U*-test are as indicated. Sample sizes for each experiment ranged from 100 to 210. (**E**) Differences in homologous pairing in the undifferentiated SH-SY5Y cells (gray bars) and the PMA-treated differentiated SH-SY5Y cells (white bars), as determined by hybridization with Vysis LSI G*ABRB3* FISH probes. Pairing was scored as homologous FISH signals with distances $\leq$2 μm apart. The bars indicate the mean ± SEM of three replicate experiments, in each of which 100–150 nuclei were scored. (**F**) The PMA-treated differentiated SH-SY5Y cells treated for 4 h with the transcriptional inhibitor, α-amanitin, were hybridized with Vysis LSI G*ABRB3* (left panel) and CEP15 (right panel) FISH probes and signals measured. Transcriptional inhibition resulted in a significant reduction in the homologous pairing at *GABRB3*, but not at CEP15. Student's *t*-test.

expression patterns within 15q11–q13. Indeed, our prior study showed that various autosomal imbalances commonly affect neuronal differentiation through the dysregulation of gene expression (37).

In this study, we made use of MMCT to generate a 15q11–q13 maternal duplication model in a neuronal cell line to explore the molecular basis of epigenetic dysregulation in 15q dup syndrome. Using this MMCT method, a maternal

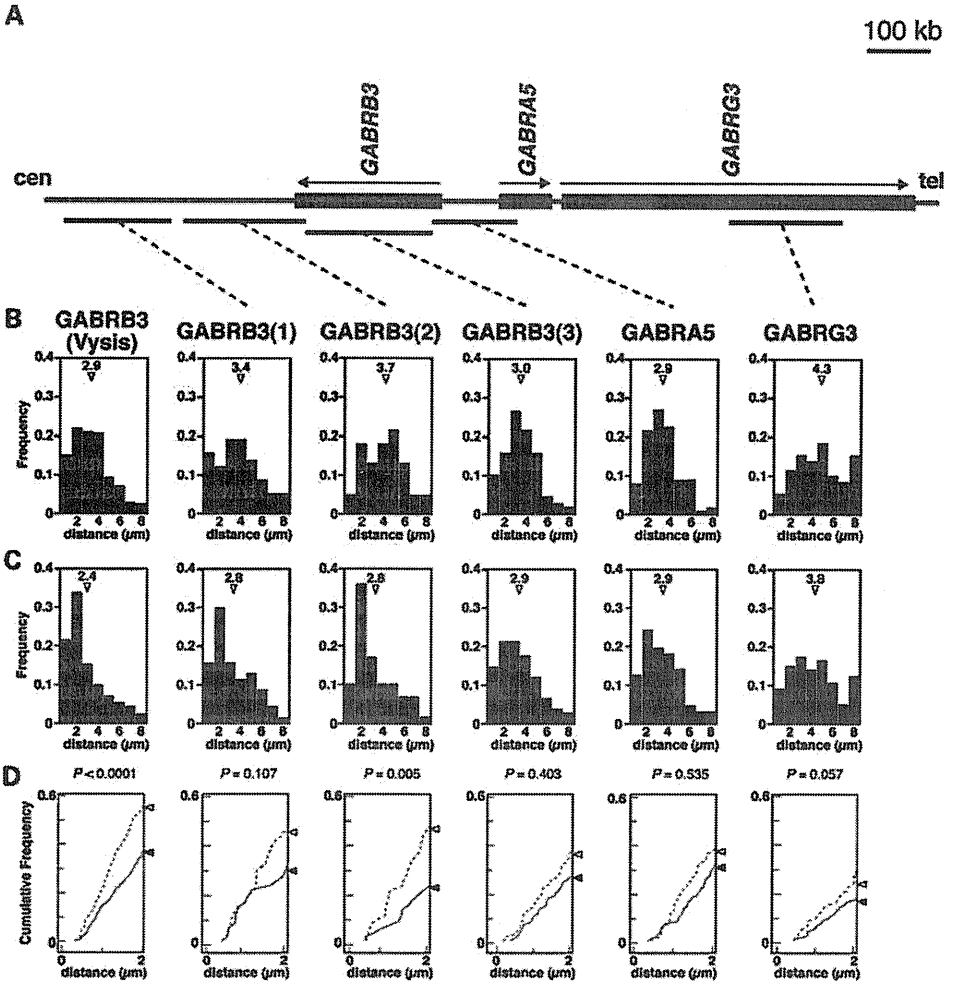

Figure 5. Homologous pairing of 15q11–q13 maps to the 3′ region of *GABRB3*. (**A**) Physical map of the cluster of $GABA_AR$ subunit genes in 15q11–q13. The genes are drawn approximately to scale. The direction of transcription is indicated by arrows. The BAC probes used in the pairing analyses are shown by horizontal bars. (**B**) Frequency distributions of distances between homologous alleles at multiple sites along 15q11–q13 for undifferentiated SH-SY5Y cell nuclei, as measured on each BAC probe. Mean distance, open triangle. (**C**) Frequency distributions of distances between homologous alleles at multiple sites along 15q11–q13 for PMA-treated differentiated SH-SY5Y cell nuclei. A high proportion of PMA-treated differentiated SH-SY5Y cells displayed close homologous distances (≤2 μm) at *GABRB3* upon neuronal differentiation, as shown by a leftward shift in the distribution. Mean distance, open triangle. (**D**) Cumulative distance distribution for homologous alleles at 0–2 μm. The solid line indicates the undifferentiated SH-SY5Y cells. The dotted line indicates the PMA-treated differentiated SH-SY5Y cells. The closed and open triangles indicate cumulative frequency at 2 μm, respectively. The statistical relevance was assessed by a comparison of the entire histogram of measurement distributions from (B) and (C) using two non-parametric tests, namely Mann–Whitney's *U*-test and Kolmogorov–Smirnov test. *P*-values from Mann–Whitney's *U*-test are as indicated. Sample sizes for each experiment ranged from 100 to 210. One probe from the 3′ region of *GABRB3* showed significant differences in homologous intrachromosomal distance frequencies between undifferentiated SH-SY5Y cells (solid line) and the PMA-treated differentiated SH-SY5Y cells (dotted line). In contrast, one probe from the *GABRB3* gene body and two probes overlapping *GABRA5* and *GABRG3* did not show significant homologous pairing. The more centromeric GABRB3(1) probe showed a trend towards homologous pairing that was not significant.

copy of human chromosome 15 was successfully transferred into human SH-SY5Y neuronal cells. Currently, CNVs, including the 15q duplication, are beginning to provide some insights into the underlying genetic causes of neurodevelopmental disorders, in particular schizophrenia and ASD. However, the impact of CNVs on phenotypic expression remains largely unknown (38). Therefore, this study takes an important step forward by using MMCT as an important tool to define the molecular effects of CNVs in a human neuronal cell line and demonstrating that a chromosome imbalance disrupts normal homologous pairing and alters gene expression patterns.

Quantitative RT–PCR analyses revealed significant alterations in gene expression of *NDN, SNRPN, UBE3A, ATP10A, GABRB3* and *CHRNA7* in SH(15M) cells, as has previously been observed in the brains of autistic patients (18). We did not find evidence for aberrant promoter DNA methylation of these genes to explain reduced transcription. Instead, we hypothesize that higher order epigenetic alterations at the level of inter- or intra-chromosomal associations lead to transcriptional down-regulation of individual genes in the 15q11–q13 region in 15q duplication syndrome.

15q11–q13 homologous pairing appears to be a recently evolved higher order epigenetic regulatory mechanism, as it

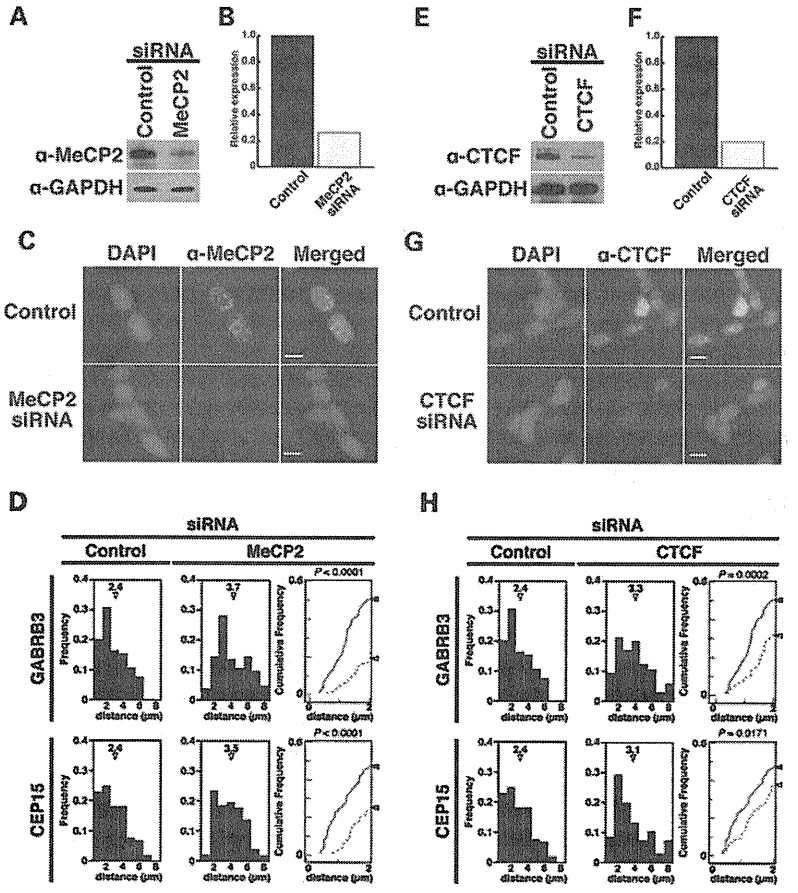

Figure 6. Disruption of *GABRB3* homologous pairing via MeCP2 and CTCF knockdown. (**A** and **E**) Results from western blot analysis confirming knockdown of MeCP2 (A) and CTCF (E) proteins in SH-SY5Y cells. (**B** and **F**) Results from western blot analysis of cell lysates after siRNA-mediated gene silencing. Both MeCP2 (B) and CTCF (F) proteins experienced ~80% knockdown. (**C** and **G**) Expression of MeCP2 (C) and CTCF (G) proteins in siRNA-treated differentiated SH-SY5Y cells. Scale bars: 10 μm. (**D** and **H**) Chr.15–Chr.15 distribution profiles and cumulative frequency curves of MeCP2 (D) and CTCF (H) in siRNA-treated differentiated SH-SY5Y cell nuclei. Mann–Whitney's *U*-test and Kolmogorov–Smirnov tests were used to determine whether the differences between the curves of the siRNA-treated cells (dotted lines) and the non-targeting siRNA-treated SH-SY5Y cells (solid lines) were significant. The statistical relevance was assessed by comparing whole histograms. *P*-values from Mann–Whitney's *U*-test are as indicated. Sample sizes for each experiment ranged from 103 to 105.

does not occur in the syntenic region in the mouse brain (20) or in lymphocytes of gorilla (39). In this study, we also found no obvious evidence for homologous pairing at the *Gabrb3* locus in mouse neurons (Supplementary Material, Fig. S5). As previously suggested elsewhere, the most likely explanation for this discrepancy is that mouse 7qC (which is homologous to the 15q11–q13 region) is not adjacent to ribosomal DNA (rDNA) genes as it is for the acrocentric human chromosome 15 (20). In addition, the *GABRB3* minimal pairing region defined in this study is highly conserved in chimp but not in mouse. These mouse–human discrepancies could begin to explain why the mouse model of 15q duplication syndrome unexpectedly showed an autism-like phenotype upon paternal transmission in opposition to what is observed in human 15q duplication patients (40). Cumulatively, these findings suggest that there has been some divergence in the genetic and/or epigenetic mechanisms relevant to homologous pairing in the human 15q11–q13 and mouse 7qC regions with potential relevance to autism.

While the proximity of *GABRB3* to the rDNA repeats on chromosome 15 may have been important in the recent evolution of homologous pairing of this locus, our study has shown that *GABRB3* pairing cannot simply be explained as a byproduct of the perinucleolar organization of acrocentric chromosomes in humans, as has been previously suggested (39). Interestingly, while both *CEP15* and *GABRB3* regions showed pairing, the effect of additional copy number of chromosome 15 on disrupting pairing was specific to *GABRB3*, not the rDNA adjacent *CEP15*, suggesting specificity to the *GABRB3* pairing beyond the acrocentric effect. Furthermore, the single gene locus most proximal to the rDNA repeats, *CYFIP*, actually exhibited increased interchromosomal distances with SH-SY5Y differentiation, suggesting that neuronal differentiation induced dynamic locus-dependent chromatin changes that were not simply rDNA proximity effects. Lastly, while transcriptional inhibition reduced *GABRB3* pairing, it had no significant effect on pairing at *CEP15*, demonstrating that *GABRB3* pairing was an active occurrence independent from rDNA organization on human 15q11–q13.

The loss of homologous pairing in the SH(15M) neuronal model led us to investigate the mechanism of homologous pairing in the 15q11–q13 region and its relation to autism

candidate genes. We narrowed down the region of homologous pairing of 15q11–q13 to the 3′ region of the *GABRB3* gene. The *GABA$_A$R* subunit genes, which encode for subunits of the receptor for the neurotransmitter GABA, are important autism candidate genes (30). Interestingly, while *GABA$_A$R* subunit genes are biallelically expressed in normal brain samples, at least one of these transcripts showed a gain of monoallelic or biased expression in half (4/8) of brain samples from autistic individuals, suggesting underlying epigenetic dysregulation (41). The pairing region likely contains some key regulatory elements for homologous pairing of 15q11–q13 which epigenetically control gene expression in the region. Our analyses revealed discrete MeCP2 and CTCF neuronal-binding sites within the *GABRB3* pairing region were observed in this minimal homologous pairing region required for optimal 15q11–q13 pairing. Differentiated SH-SY5Y cells showed dynamic changes in chromatin structure compared with undifferentiated cells, consistent with a model of active pairing and increased transcription of *GABRB3* with differentiation. Interestingly, previous linkage analyses have shown a significant association between *GABRB3* polymorphisms and autism (42,43). One such *GABRB3* microsatellite has been localized to ~60 kb beyond the 3′ end of the *GABRB3* gene (44) that lies within the *GABRB3* minimal pairing region and interacts with the maternal PWS-IC (Supplementary Material, Fig. S6). Interestingly, maternal transmission of a rare GABRB3 signal peptide variant has been recently observed in autism (45).

Recent findings showed that CTCF and OCT4 together can mediate X-chromosome pairing, and the results of our homologous pairing analyses also suggest that CTCF can mediate specific inter-chromosomal associations in the 3′ region of the *GABRB3* gene (34). Indeed, we identified three potential CTCF-binding sites bordering the homologous pairing region. On the basis of our RNAi-mediated knockdown studies, we conclude that CTCF controls not only X chromosome pairing but also autosomal 15q11–q13 pairing. Although our study highlights CTCF as a central molecule in inter-chromosomal association, its exact role in the etiology of neurodevelopmental disorders remains uncertain. One recent study revealed that CTCF and cohesin complexes are necessary for establishing the chromatin structure required for brain-derived neurotrophic factor transcription (46). Thus, there is already some evidence indicating how epigenetic factors such as CTCF and MeCP2 may play a role in complex psychiatric and neurodevelopmental disorders (16).

It is plausible that MeCP2, such as CTCF, also controls the homologous pairing of 15q11–q13. Mutations in *MECP2* cause RTT, a neurodevelopmental disorder characterized by the loss of speech and acquired motor skills, stereotypical hand movements, and seizures during early childhood (47). In addition, *MECP2* mutations have been found in a few patients diagnosed with AS and autism, suggesting overlap in the pathogenesis of these distinct genetic syndromes (48,49). Consistent with phenotypic and genetic overlap among RTT, AS and autism patients, one previous study demonstrated significant defects in the expression of *UBE3A* and *GABRB3* in brain samples from RTT, AS and autism patients (50). Consistent with results of a previous study utilizing an oligonucleotide decoy approach, we demonstrated that homologous pairing at the *GABRB3* locus was significantly impacted by siRNA-mediated MeCP2 knockdown (20). This finding suggests that inter-chromosomal associations such as homologous pairing are essential for precise gene expression of *GABRB3* during neuronal differentiation. Further experiments are needed to determine how homologous pairing controls the expression of *GABRB3* transcripts. In a simple model, homologous 15q11–q13 pairing might provide a transcriptionally positive environment by recruiting homologous alleles at the same transcription factory to increase neuronal gene expression by recycling positive factors at both alleles. Indeed, the transcriptional inhibitor α-amanitin caused a significant decrease in the homologous 15q11–q13 pairing, further demonstrating the requirement of active transcription for homologous 15q11–q13 pairing.

Recently, development of new techniques such as the chromosomal conformation capture (3C) assay has enabled description of long-range intra-chromosomal associations, such as those at the *H19-Igf2* and *Dlx5/Dlx6* loci (51,52). Similar intra-chromosomal associations have been proposed in the regulation of 15q11–q13 genes because PWS-IC acts in *cis* to regulate paternal expression of *MKRN3*, *MAGEL2*, *NDN* and *SNRPN* genes within 15q11–q13 (53). In support of this hypothesis, our DNA-RNA FISH results showed that the PWS-IC makes an allele-specific association with the homologous pairing region of the *GABRB3* locus in differentiated SH-SY5Y cells (Supplementary Material, Fig. S6). These results may indicate that the intra-chromosomal association between the PWS-IC and *GABRB3* occurs on the maternal 15q11–q13 allele. On the other hand, disassociation of the PWS-IC and *GABRB3* is consistent with paternal allele-specific decondensation of chromatin at this locus during neuronal maturation (54). We speculate that maternal 15q duplication might alter the intrachromosomal association between the PWS-IC and *GABRB3*, thus disrupting the coordinated gene regulation of 15q11–q13.

In conclusion, 15q11–q13 appears to be a useful model region for studying epigenetic pathways and mechanisms such as long-range chromatin organization and homologous pairing. Our observations imply that CNVs such as 15q duplication alter such epigenetic mechanisms, thus disrupting regulation of individual genes at the level of inter- and intra-chromosomal associations. In order to fully understand how CNVs affect the nucleus on a molecular level, it will be important to define chromosomal regulatory elements using diverse genetic approaches, such as MMCT. Furthermore, the characterization of MeCP2 as well as CTCF can reveal additional partners involved in regulation of inter- or intra-chromosomal associations. The investigation of such interplaying partners will help in designing potential drug targets, enabling the development of a therapeutic approach for the treatment of dup15q syndrome.

MATERIALS AND METHODS

Cell lines

A9 hybrids containing a maternal human chromosome 15 tagged with pST*neo* were constructed as previously described (55) and were cultured in Dulbecco's modified Eagle medium (DMEM) (WAKO, Tokyo, Japan) supplemented with 10% calf serum (Hyclone, Thermo Scientific, Waltham, MA,

USA) and 800 μg/ml G418 (Nakarai, Kyoto, Japan). SH-SY5Y neuroblastoma cells (ATCC, USA) were cultured in the DMEM/F12 medium (WAKO) supplemented with 15% fetal bovine serum (Hyclone, Thermo Scientific). For FISH analysis, cells were seeded onto Lab-Tek™ II-CC2™ Chamber Slides (Nalge Nunc, Penfield, NY, USA) and grown until they reached 30–50% confluency. Cells were fixed either before (untreated) or 72 h after the addition of 16 nM PMA (PMA treated) for 15 min in Histochoice (Amresco, Solon, OH, USA) and then washed in 1× PBS/0.5% Tween 20 for 5 min and stored in 70% ethanol at −20°C. For α-amanitin experiments, PMA-treated SH-SY5Y cells were treated with 20 or 30 μg/ml α-amanitin for 4 h.

Microcell-mediated chromosome transfer

Introduction of an extra maternal human chromosome 15 into human SH-SY5Y neuronal cells was performed via MMCT, as previously described (56). Briefly, microcells purified from 1 × 10^8 donor A9 cells containing a maternal human chromosome 15 were fused with SH-SY5Y cells using 47% polyethylene glycol 1000 (PEG1000: Mr 1000; Nakarai). SH-SY5Y microcell hybrid clones were selected individually in the DMEM/F12 medium supplemented with 15% FBS and 600 μg/ml of G418 for 2–3 weeks. These clones were usually maintained stably in culture under appropriate selective conditions. The introduction of maternal human chromosome 15 in SH-SY5Y cells was confirmed by PCR-RFLP analysis and cytogenetic analysis. The primers for RFLP analysis were 5′-AGTGGGCTTCCCTCACTTCT-3′ (forward) and 5′-CAGACAGGCTCCACTTACCC-3′ (reverse). Three independent SH-SY5Y cells with an extra maternal human chromosome 15 obtained from each chromosome transfer were selected for further expression and pairing analyses.

Cytogenetic analysis

To confirm the presence of the transferred human chromosome 15 in SH-SY5Y cells, FISH analysis was performed on fixed metaphase spreads of each SH-SY5Y clone using the Vysis LSI Prader-Willi/Angelman Region Probe (GABRB3) (Abbott, North Chicago, IL, USA), as described previously (21). Chromosomes were counterstained with DAPI (Sigma, St Louis, MO, USA).

FISH and pairing assays

DNA FISH analysis was performed as described previously (54). Briefly, FISH was conducted in SH-SY5Y neuroblasts and SH-SY5Y neurons differentiated by 72 h treatment with 16 nM PMA (20). FISH probes for *GABRB3* and *CEP15* were obtained commercially from Vysis, but to determine precise locations of pairing, BAC probes were obtained (CHORI, Oakland, CA, USA). BAC DNA was labeled with Green-dUTP or Orange-dUTP (Abbott). BAC clones for FISH are as follow; RP11-69H14 (*CYFIP1*), RP11-373J1 (*NDN*), RP11-125E1 (*SNRPN*), RP11-171C8 (*HBII-85*), RP11-1081A4 (*UBE3A*), RP11-339C21 (*ATP10A*), RP11-92F7 (*TJP1*), RP11-714E8 (*CHRNA7*), RP11-638J6 (*GABRB3*(1)), RP11-345N11 (*GABRB3*(2)), RP11-974L14 (*GABRB3*(3)), RP11-243J20 (*GABRA5*), RP11-89E18 (*GABRG3*), RP11-79M7 (*GABRG1*), RP11-905L4 (*GABRA2*), RP11-620L1 (*GABRA4*), RP11-1059P8 (*GABRB1*), RP11-315P17 (*GABRB2*(1)), RP11-833C4 (*GABRB2*(2)), RP11-348M17 (*GABRA1*), RP11-204E3 (*GABRG2*), RP23-24D4 (*Gabrb3*, I), RP23-143O21 (*Gabrb3*, II) and RP23-459J11 (*Gabrb3*, III). A nick translation kit (Roche, Penzberg, Germany) was used to create probes, which were then hybridized to cells fixed in Histochoice (Amresco), then dehydrated in 70, 90 and 100% ethanol (10 min each) and dried at 50°C. FISH probes were denatured with the fixed cells at 80°C for 2 min and then hybridized overnight at 37°C on cover-slipped slides. Cells were washed three times in 50% formamide/50% 2× SSC for 5 min, 2× SSC for 5 min and 2× SSC/0.1% IGEPAL for 5 min at 46°C and then mounted in Vectashield (Vector Laboratories, Burlingame, CA, USA) containing 5 μg/μl DAPI. To analyze pairing, we took digital images with a BX51 fluorescence microscope (Olympus, Tokyo, Japan) equipped with a RETIGA EXi CCD camera (Qimaging, Surrey, Canada); these were processed in iVision 4.0 software (BioVision Technologies, Exton, PA, USA). The iVision software was also used to measure distances between two signals. All FISH distances are measured in 2D in this study because 3D is less of a concern for neurons, which are relatively flat compared with round nuclei seen in lymphocytes. Although 2D may change some measurements, signals that are significantly closer than expected of random were likely to be close in 3D space. To simplify the analysis of homologous association or 'pairing' as has been described previously (19,20), nuclei with FISH signals ≤2 μm apart were scored as 'paired', while nuclei with two FISH signals >2 μm apart were scored as 'unpaired'. In case of SH(15M) cells, we measured the shortest inter-chromosomal distances between the three signals. Measurement and scoring of FISH signals were performed manually and results are averages of at least three independent scores per sample.

Gene expression analysis

Total RNA was extracted using RNeasy columns, according to the manufacturer's protocols (Qiagen, Hilden, Germany) and then treated with RNase-free DNase I (Takara, Kyoto, Japan). First-strand cDNA synthesis was carried out with random primers and SuperScript® III reverse transcriptase (Invitrogen, Carlsbad, CA, USA). Quantitative RT–PCR was performed with GoTaq® qPCR Master Mix (Promega, Fitchburg, WI, USA) on a CFX384 Real-Time PCR Detection System (Bio-Rad, Hercules, CA, USA). Three replicate reactions were conducted for each gene analyzed. Melting curve analysis was performed to ensure that a single product was amplified with each primer set. Relative expression levels of 15q11–q13 transcripts were normalized by using the comparative Ct (ΔΔCt) method and the geometric average of a set of two housekeeping genes (*GAPDH* and *ACTB*) by the Bio-Rad CFX manager software (version 1.5). Primer sequences are available on request.

RNAi knockdown

We carried out siRNA-mediated knockdown of MeCP2, CTCF and RAD21 proteins using Accell SMART pool siRNAs,

according to the manufacturer's protocols (Dharmacon, Lafayette, CO, USA). Accell non-targeting siRNA was used in control knockdowns. Briefly, we plated SH-SY5Y cells onto Lab-Tek™ II-CC2™ Chamber Slides (Nalge Nunc) and then incubated them for 72 h in serum-free Accell SMART pool transfection medium containing 1 μM of MeCP2, CTCF or RAD21 siRNAs. After 72 h of siRNA treatment, we replaced the medium with 1% serum-supplemented Accell medium containing 16 nm PMA and a pool of each siRNA, as appropriate. For pairing analysis and knockdown assessment, cells were fixed in Histochoice (Amresco) or harvested after an additional 72 h of incubation. MeCP2, CTCF and RAD21 knockdowns were confirmed by western blot analysis using rabbit anti-MeCP2 (Diagenode, Sparta, NJ, USA), rabbit anti-CTCF (CST, Danvers, MA, USA), rabbit anti-RAD21 (CST) and rabbit anti-GAPDH (CST), with the appropriate rabbit secondary antibodies conjugated to horseradish peroxidase for detection (Bio-Rad). Immunostaining was conducted with anti-MeCP2, anti-CTCF and anti-RAD21, and detection was achieved with secondary Alexa Fluor 555-goat anti-rabbit or Alexa Fluor 488-goat anti-rabbit (Invitrogen).

DNA methylation analysis

We performed DNA methylation analysis using EpiTect® Bisulfite Kits (Qiagen), according to the manufacturer's protocols. Specific primers for the amplification of bisulfite-treated DNA were designed using MethPrimer (http://www.urogene.org/methprimer). PCR was performed using GoTaq® Master Mix (Promega). PCR conditions were as follows: 2 min hot start at 95°C, followed by 32 cycles of denaturation at 95°C for 30 s, annealing at 58°C for 30 s and extension at 72°C for 30 s. The PCR products were directly cloned into the pGEM®-T Easy vector (Promega). Twenty individual clones were sequenced from both ends using a 310 Genomic Analyzer (Applied Biosystems Inc., Foster City, CA, USA) according to the standard protocols. Primer sequences are available on request.

Chromatin immunoprecipitation

Chromatin was prepared from SH-SY5Y cells and purified by urea gradient centrifugation, as previously described (52). Immunoprecipitation, reverse crosslinking and PCR amplification were also performed as previously described (52), with some modifications. Briefly, a panel of restriction enzymes (NEB, Ipswich, MA, USA) was used to digest chromatin into 100–700 bp DNA fragments. Digested chromatin was pre-cleared with Protein G Dynabeads (Invitrogen) alone, then with normal rabbit IgG (CST) and then finally with Protein G Dynabeads. Pre-cleared chromatin was incubated overnight with rabbit anti-CTCF or with equivalent amounts of normal rabbit IgG as a control for non-specific binding. PCR amplification was performed for 35 cycles with one-twentieth of the IP products. Primer sequences are available on request.

SUPPLEMENTARY MATERIAL

Supplementary Material is available at *HMG* online.

ACKNOWLEDGEMENTS

We thank Karen N. Leung for her advice on FISH protocols and Masako Tada, Hiroyuki Kugoh for critical reading of the manuscript. We would also like to thank Sachiyo Akagi and Miwa Miyano for their help with the MMCT and PCR analysis.

Conflict of Interest statement. None declared.

FUNDING

This work was supported in part by Grants-in-Aid for JSPS Fellows and a Short-term Fellowship from the International Human Frontier Science Program (M.M.-H.), the Program for Improvement of Research Environment for Young Researchers from the Special Coordination Funds for Promoting Science and Technology (S.H.), Grant-in-Aid for Scientific Research on Priority Areas (S.H.), Grants-in-Aid for Scientific Research on Innovative Areas (S.H.), Grants-in-Aid for Young Scientists (B) (S.H.), The Cell Science Research Foundation, Daiichi-Sankyo Foundation of Life Science, Mitsubishi Pharma Research Foundation and Life Science Foundation of Japan (S.H.), the Program for Promotion of Basic and Applied Researches for Innovations in Bio-oriented Industry (H.I., S.H.) and the National Institutes of Health (J.M.L., R01HD048799 and R01HD41462).

REFERENCES

1. Folstein, S.E. and Rosen-Sheidley, B. (2001) Genetics of autism: complex aetiology for a heterogeneous disorder. *Nat. Rev. Genet.*, **2**, 943–955.
2. Fombonne, E. (2003) Epidemiological surveys of autism and other pervasive developmental disorders: an update. *J. Autism Dev. Disord.*, **33**, 365–382.
3. Cook, E.H. Jr. and Scherer, S.W. (2008) Copy-number variations associated with neuropsychiatric conditions. *Nature*, **455**, 919–923.
4. Pinto, D., Pagnamenta, A.T., Klei, L., Anney, R., Merico, D., Regan, R., Conroy, J., Magalhaes, T.R., Correia, C., Abrahams, B.S. *et al.* (2010) Functional impact of global rare copy number variation in autism spectrum disorders. *Nature*, **466**, 368–372.
5. Wang, N.J., Liu, D., Parokonny, A.S. and Schanen, N.C. (2004) High-resolution molecular characterization of 15q11-q13 rearrangements by array comparative genomic hybridization (array CGH) with detection of gene dosage. *Am. J. Hum. Genet.*, **75**, 267–281.
6. Cook, E.H. Jr, Lindgren, V., Leventhal, B.L., Courchesne, R., Lincoln, A., Shulman, C., Lord, C. and Courchesne, E. (1997) Autism or atypical autism in maternally but not paternally derived proximal 15q duplication. *Am. J. Hum. Genet.*, **60**, 928–934.
7. Schroer, R.J., Phelan, M.C., Michaelis, R.C., Crawford, E.C., Skinner, S.A., Cuccaro, M., Simensen, R.J., Bishop, J., Skinner, C., Fender, D. *et al.* (1998) Autism and maternally derived aberrations of chromosome 15q. *Am. J. Med. Genet*, **76**, 327–336.
8. Lauritsen, M., Mors, O., Mortensen, P.B. and Ewald, H. (1999) Infantile autism and associated autosomal chromosome abnormalities: a register-based study and a literature survey. *J. Child Psychol. Psychiatry*, **40**, 335–345.
9. Veenstra-Vanderweele, J., Christian, S.L. and Cook, E.H. Jr. (2004) Autism as a paradigmatic complex genetic disorder. *Annu. Rev. Genomics Hum. Genet.*, **5**, 379–405.
10. Szatmari, P., Paterson, A.D., Zwaigenbaum, L., Roberts, W., Brian, J., Liu, X.Q., Vincent, J.B., Skaug, J.L., Thompson, A.P., Senman, L. *et al.* (2007) Mapping autism risk loci using genetic linkage and chromosomal rearrangements. *Nat. Genet.*, **39**, 319–328.

11. Knoll, J.H., Nicholls, R.D., Magenis, R.E., Graham, J.M. Jr, Lalande, M. and Latt, S.A. (1989) Angelman and Prader-Willi syndromes share a common chromosome 15 deletion but differ in parental origin of the deletion. *Am. J. Med. Genet.*, **32**, 285–290.
12. Reik, W. and Walter, J. (2001) Genomic imprinting: parental influence on the genome. *Nat. Rev. Genet.*, **2**, 21–32.
13. Kishino, T., Lalande, M. and Wagstaff, J. (1997) UBE3A/E6-AP mutations cause Angelman syndrome. *Nat. Genet.*, **15**, 70–73.
14. Matsuura, T., Sutcliffe, J.S., Fang, P., Galjaard, R.J., Jiang, Y.H., Benton, C.S., Rommens, J.M. and Beaudet, A.L. (1997) De novo truncating mutations in E6-AP ubiquitin-protein ligase gene (UBE3A) in Angelman syndrome. *Nat. Genet.*, **15**, 74–77.
15. Jiang, Y.H., Sahoo, T., Michaelis, R.C., Bercovich, D., Bressler, J., Kashork, C.D., Liu, Q., Shaffer, L.G., Schroer, R.J., Stockton, D.W. *et al.* (2004) A mixed epigenetic/genetic model for oligogenic inheritance of autism with a limited role for UBE3A. *Am. J. Med. Genet. A*, **131**, 1–10.
16. Schanen, N.C. (2006) Epigenetics of autism spectrum disorders. *Hum. Mol. Genet.*, **15**, R138–R150.
17. Grafodatskaya, D., Chung, B., Szatmari, P. and Weksberg, R. (2010) Autism spectrum disorders and epigenetics. *J. Am. Acad. Child Adolesc. Psychiatry*, **49**, 794–809.
18. Hogart, A. and LaSalle, J.M. (2009) Chromosome 15q11–13 duplication syndrome brain reveals epigenetic alterations in gene expression not predicted from copy number. *J. Med. Genet.*, **46**, 86–93.
19. LaSalle, J.M. and Lalande, M. (1996) Homologous association of oppositely imprinted chromosomal domains. *Science*, **272**, 725–728.
20. Thatcher, K.N., Peddada, S., Yasui, D.H. and Lasalle, J.M. (2005) Homologous pairing of 15q11–13 imprinted domains in brain is developmentally regulated but deficient in Rett and autism samples. *Hum. Mol. Genet.*, **14**, 785–797.
21. Kugoh, H., Mitsuya, K., Meguro, M., Shigenami, K., Schulz, T.C. and Oshimura, M. (1999) Mouse A9 cells containing single human chromosomes for analysis of genomic imprinting. *DNA Res.*, **6**, 165–172.
22. Mitsuya, K., Meguro, M., Lee, M.P., Katoh, M., Schulz, T.C., Kugoh, H., Yoshida, M.A., Niikawa, N., Feinberg, A.P. and Oshimura, M. (1999) LIT1, an imprinted antisense RNA in the human KvLQT1 locus identified by screening for differentially expressed transcripts using monochromosomal hybrids. *Hum. Mol. Genet.*, **8**, 1209–1217.
23. Meguro, M., Mitsuya, K., Nomura, N., Kohda, M., Kashiwagi, A., Nishigaki, R., Yoshioka, H., Nakao, M., Oishi, M. and Oshimura, M. (2001) Large-scale evaluation of imprinting status in the Prader-Willi syndrome region: an imprinted direct repeat cluster resembling small nucleolar RNA genes. *Hum. Mol. Genet.*, **10**, 383–394.
24. Nakabayashi, K., Bentley, L., Hitchins, M.P., Mitsuya, K., Meguro, M., Minagawa, S., Bamforth, J.S., Stanier, P., Preece, M., Weksberg, R. *et al.* (2002) Identification and characterization of an imprinted antisense RNA (MESTIT1) in the human MEST locus on chromosome 7q32. *Hum. Mol. Genet.*, **11**, 1743–1756.
25. Pahlman, S., Hoehner, J.C., Nanberg, E., Hedborg, F., Fagerstrom, S., Gestblom, C., Johansson, I., Larsson, U., Lavenius, E., Ortoft, E. *et al.* (1995) Differentiation and survival influences of growth factors in human neuroblastoma. *Eur. J. Cancer*, **31A**, 453–458.
26. Spengler, B.A., Biedler, J.L. and Ross, R.A. (2002) A corrected karyotype for the SH-SY5Y human neuroblastoma cell line. *Cancer Genet. Cytogenet.*, **138**, 177–178.
27. El-Maarri, O., Buiting, K., Peery, E.G., Kroisel, P.M., Balaban, B., Wagner, K., Urman, B., Heyd, J., Lich, C., Brannan, C.I. *et al.* (2001) Maternal methylation imprints on human chromosome 15 are established during or after fertilization. *Nat. Genet.*, **27**, 341–344.
28. Jay, P., Rougeulle, C., Massacrier, A., Moncla, A., Mattei, M.G., Malzac, P., Roëckel, N., Taviaux, S., Lefranc, J.L., Cau, P. *et al.* (1997) The human necdin gene, NDN, is maternally imprinted and located in the Prader-Willi syndrome chromosomal region. *Nat. Genet.*, **17**, 357–361.
29. Xiong, Z. and Laird, P.W. (1997) COBRA: a sensitive and quantitative DNA methylation assay. *Nucleic Acids Res.*, **25**, 2532–2534.
30. Hogart, A. and LaSalle, J.M. (2010) Epigenetic Dysregulation of 15q11–13 GABAA Receptor Genes in Autism. In *The Neurochemical Basis of Autism*, Springer, pp. 113–127.
31. Kurukuti, S., Tiwari, V.K., Tavoosidana, G., Pugacheva, E., Murrell, A., Zhao, Z., Lobanenkov, V., Reik, W. and Ohlsson, R. (2006) CTCF binding at the H19 imprinting control region mediates maternally inherited higher-order chromatin conformation to restrict enhancer access to Igf2. *Proc. Natl Acad. Sci. USA*, **103**, 10684–10689.
32. Ohlsson, R., Bartkuhn, M. and Renkawitz, R. (2010) CTCF shapes chromatin by multiple mechanisms: the impact of 20 years of CTCF research on understanding the workings of chromatin. *Chromosoma*, **119**, 351–360.
33. Williams, A. and Flavell, R.A. (2008) The role of CTCF in regulating nuclear organization. *J. Exp. Med.*, **205**, 747–750.
34. Donohoe, M.E., Silva, S.S., Pinter, S.F., Xu, N. and Lee, J.T. (2009) The pluripotency factor Oct4 interacts with Ctcf and also controls X-chromosome pairing and counting. *Nature*, **460**, 128–132.
35. Wendt, K.S., Yoshida, K., Itoh, T., Bando, M., Koch, B., Schirghuber, E., Tsutsumi, S., Nagae, G., Ishihara, K., Mishiro, T. *et al.* (2008) Cohesin mediates transcriptional insulation by CCCTC-binding factor. *Nature*, **451**, 796–801.
36. Herzing, L.B., Cook, E.H. Jr. and Ledbetter, D.H. (2002) Allele-specific expression analysis by RNA-FISH demonstrates preferential maternal expression of UBE3A and imprint maintenance within 15q11-q13 duplications. *Hum. Mol. Genet.*, **11**, 1707–1718.
37. Kai, Y., Wang, C.C., Kishigami, S., Kazuki, Y., Abe, S., Takiguchi, M., Shirayoshi, Y., Inoue, T., Ito, H., Wakayama, T. *et al.* (2009) Enhanced apoptosis during early neuronal differentiation in mouse ES cells with autosomal imbalance. *Cell Res.*, **19**, 247–258.
38. Lee, C. and Scherer, S.W. (2010) The clinical context of copy number variation in the human genome. *Expert Rev. Mol. Med.*, **12**, e8.
39. Teller, K., Solovei, I., Buiting, K., Horsthemke, B. and Cremer, T. (2007) Maintenance of imprinting and nuclear architecture in cycling cells. *Proc. Natl Acad. Sci. USA*, **104**, 14970–14975.
40. Nakatani, J., Tamada, K., Hatanaka, F., Ise, S., Ohta, H., Inoue, K., Tomonaga, S., Watanabe, Y., Chung, Y.J., Banerjee, R. *et al.* (2009) Abnormal behavior in a chromosome-engineered mouse model for human 15q11–13 duplication seen in autism. *Cell*, **137**, 1235–1246.
41. Hogart, A., Nagarajan, R.P., Patzel, K.A., Yasui, D.H. and Lasalle, J.M. (2007) 15q11–13 GABAA receptor genes are normally biallelically expressed in brain yet are subject to epigenetic dysregulation in autism-spectrum disorders. *Hum. Mol. Genet.*, **16**, 691–703.
42. Cook, E.H. Jr, Courchesne, R.Y., Cox, N.J., Lord, C., Gonen, D., Guter, S.J., Lincoln, A., Nix, K., Haas, R., Leventhal, B.L. *et al.* (1998) Linkage-disequilibrium mapping of autistic disorder, with 15q11–13 markers. *Am. J. Hum. Genet.*, **62**, 1077–1083.
43. Buxbaum, J.D., Silverman, J.M., Smith, C.J., Greenberg, D.A., Kilifarski, M., Reichert, J., Cook, E.H. Jr, Fang, Y., Song, C.Y. and Vitale, R. (2002) Association between a GABRB3 polymorphism and autism. *Mol. Psychiatry*, **7**, 311–316.
44. Martin, E.R., Menold, M.M., Wolpert, C.M., Bass, M.P., Donnelly, S.L., Ravan, S.A., Zimmerman, A., Gilbert, J.R., Vance, J.M., Maddox, L.O. *et al.* (2000) Analysis of linkage disequilibrium in gamma-aminobutyric acid receptor subunit genes in autistic disorder. *Am. J. Med. Genet.*, **96**, 43–48.
45. Delahanty, R.J., Kang, J.Q., Brune, C.W., Kistner, E.O., Courchesne, E., Cox, N.J., Cook, E.H. Jr., Macdonald, R.L. and Sutcliffe, J.S. (2011) Maternal transmission of a rare GABRB3 signal peptide variant is associated with autism. *Mol. Psychiatry*, **16**, 86–96.
46. Chang, J., Zhang, B., Heath, H., Galjart, N., Wang, X. and Milbrandt, J. (2010) Nicotinamide adenine dinucleotide (NAD)-regulated DNA methylation alters CCCTC-binding factor (CTCF)/cohesin binding and transcription at the BDNF locus. *Proc. Natl Acad. Sci. USA*, **107**, 21836–21841.
47. Amir, R.E., Van den Veyver, I.B., Wan, M., Tran, C.Q., Francke, U. and Zoghbi, H.Y. (1999) Rett syndrome is caused by mutations in X-linked MECP2, encoding methyl-CpG-binding protein 2. *Nat. Genet.*, **23**, 185–188.
48. Watson, P., Black, G., Ramsden, S., Barrow, M., Super, M., Kerr, B. and Clayton-Smith, J. (2001) Angelman syndrome phenotype associated with mutations in MECP2, a gene encoding a methyl CpG binding protein. *J. Med. Genet.*, **38**, 224–228.
49. Lam, C., Yeung, W., Ko, C., Poon, P., Tong, S., Chan, K., Lo, I., Chan, L., Hui, J., Wong, V. *et al.* (2000) Spectrum of mutations in the MECP2 gene in patients with infantile autism and Rett syndrome. *J. Med. Genet.*, **37**, E41.
50. Samaco, R.C., Hogart, A. and LaSalle, J.M. (2005) Epigenetic overlap in autism-spectrum neurodevelopmental disorders: MECP2 deficiency

causes reduced expression of UBE3A and GABRB3. *Hum. Mol. Genet.*, **14**, 483–492.
51. Murrell, A., Heeson, S. and Reik, W. (2004) Interaction between differentially methylated regions partitions the imprinted genes Igf2 and H19 into parent-specific chromatin loops. *Nat. Genet.*, **36**, 889–893.
52. Horike, S., Cai, S., Miyano, M., Cheng, J.F. and Kohwi-Shigematsu, T. (2005) Loss of silent-chromatin looping and impaired imprinting of DLX5 in Rett syndrome. *Nat. Genet.*, **37**, 31–40.
53. Yang, T., Adamson, T.E., Resnick, J.L., Leff, S., Wevrick, R., Francke, U., Jenkins, N.A., Copeland, N.G. and Brannan, C.I. (1998) A mouse model for Prader-Willi syndrome imprinting-centre mutations. *Nat. Genet.*, **19**, 25–31.
54. Leung, K.N., Vallero, R.O., DuBose, A.J., Resnick, J.L. and LaSalle, J.M. (2009) Imprinting regulates mammalian snoRNA-encoding chromatin decondensation and neuronal nucleolar size. *Hum. Mol. Genet.*, **18**, 4227–4238.
55. Inoue, J., Mitsuya, K., Maegawa, S., Kugoh, H., Kadota, M., Okamura, D., Shinohara, T., Nishihara, S., Takehara, S., Yamauchi, K. *et al.* (2001) Construction of 700 human/mouse A9 monochromosomal hybrids and analysis of imprinted genes on human chromosome 6. *J. Hum. Genet.*, **46**, 137–145.
56. Koi, M., Shimizu, M., Morita, H., Yamada, H. and Oshimura, M. (1989) Construction of mouse A9 clones containing a single human chromosome tagged with neomycin-resistance gene via microcell fusion. *Jpn. J. Cancer Res.*, **80**, 413–418.